STM JOURNALS

Journal of
Nuclear Engineering & Technology

ISSN: 2277-6184 (Online)
ISSN: 2321-6514 (Print)
Volume 16, Issue 1, 2026
January–April
DOI (Journal): 10.37591/JoNET

https://journals.stmjournals.com/jonet

Research JoNET

Theoretical Study of Z = 122 Nuclei

Santosh Kumar[1,*], S.K. Singh[2]

Abstract

We used atomic nuclei with proton number Z = 122 to calculate bulk properties within the relativistic mean field (RMF) theory. We utilized the force parameters recognized as NL3 in our calculations. We extend our calculation to isotopic series of Z = 122 and analyze the theoretical outcomes. A whole isotopic chain of nuclei with atomic number Z = 122 Z=122 is included in our inquiry, enabling a methodical examination of their structural evolution as a function of neutron number. We compute key bulk nuclear parameters, such as total binding energy, root mean square (rms) matter radius, and charge distribution radius, for every isotope in this series. These observables offer important information about the size, distribution, and stability of nuclear matter in superheavy systems. By computing the alpha-decay half-lives, we investigate the decay behavior of the Z=122 and Z=122 isotopes in addition to their ground-state characteristics. The consistency and dependability of our results are evaluated by comparing the estimated half-life values with predictions derived from well-established theoretical models. Understanding the stability and decay mechanisms of superheavy nuclei, where experimental data are still incredibly scarce, depends on these similarities. All things considered, the current study advances our theoretical knowledge of the structural characteristics and decay patterns of nuclei with Z = 122 Z=122 and offers helpful direction for next theoretical and experimental studies in the field of superheavy elements. For isotopic families of nuclei with atomic number Z = 122, we initiated calculations of fundamental bulk properties like binding energy, root mean square radius, and charge distribution radius. We also calculate the half-life of an alpha particle and compare it with the established theoretical models.

Keywords: Binding energy, charge distribution, half-life, Q_α, relativistic mean field, Thomas–Fermi approximation

INTRODUCTION

A superheavy element designated as Z = 122 refers to a theoretical element that is frequently anticipated to reside within the region known as the "island of stability" among superheavy nuclei [1]. The investigation of superheavy elements has fascinated both theoretical and experimental researchers. When two heavy ions collide, a fusion process occurs, leading to the formation of superheavy elements. Current studies characterize fusion in two ways: as the movement of nucleons or clusters from a lighter nucleus to a heavier one, or as the combination of two nuclei based on their spatial arrangement [2]. Due to the substantial positive charge of the very heavy elements, Coulombic repulsion occurs within the nucleus. The "island of stability" is located in the Z = 114 − 126 region, where certain superheavy nuclei (SHN) exhibit longer half-lives and are relatively more stable. Intense repulsion occurs in the nucleus because of the strong force operating there, which has a limited range owing to the diminished nuclear binding energy. Decay is favored because the energy equilibrium occurs in the superheavy element. This energy balance aids both alpha-decay and spontaneous fission.

In a foundational study [3] that investigated the interaction of ^{238}U with a ^{nat}Zn target, the researchers noted the emergence of both fusion-

***Author for Correspondence**
Santosh Kumar
E-mail: sankm036@gmail.com

[1]Research Scholar, Department of Physics, Patliputra University, Patna, Bihar, India.
[2]Faculty, Department of Physics, Patliputra University, Patna, Bihar, India.

Received Date: December 16, 2025
Accepted Date: December 30, 2025
Published Date: January 01, 2026

Citation: Santosh Kumar, S.K. Singh. Reimagining Nuclear Reactor Safety: Theoretical Study of Z = 122 Nuclei. Journal of Nuclear Engineering & Technology. 2026; 16(1): 1–9p.

fission (ff) and quasi-fission (qf) phenomena in the exceptionally heavy nucleus $^{302}122$. This occurred at bombarding energies of 5.4, 6.7, and 7.5 MeV per nucleon, which corresponded to excitation energies of the compound nucleus (E^*) of 27, 93, and 133 MeV, respectively. More recently, "hot" fusion reactions such as $^{58}Fe + {}^{248}Cm \rightarrow 306122^*$ and $^{64}Ni + {}^{242}Pu \rightarrow 306122^*$ at an excitation energy (E^*) of 33 MeV have evidenced these same two mechanisms [4]. Manjunatha [5] studied the theoretical expectations regarding potential isotopes of the superheavy element with atomic number Z = 122.

The findings indicated that isotopes $^{307–314}122$ have significantly long half-lives, making it feasible to detect them if they are successfully created in a laboratory setting.

In the present investigation, we examine the macroscopic characteristics, such as binding energy, charge radius, root mean square radius, neutron skin thickness, and half-life associated with α decay processes of the nucleus with atomic number Z = 122, employing the highly successful NL3 force parameter with relativistic extended Thomas–Fermi (RETF).

The following description details the structure of this paper: The binding energy of isotopes with Z = 122 is calculated using the NL3 force parameter set [6] in the context of relativistic mean field (RMF) theory via a self-consistent iterative approach. Other observables, such as the charge radius, neutron skin thickness, and half-lives for α, were also investigated. A brief overview and related conclusions are provided in the concluding section of this paper.

THEORETICAL FORMALISM

Within the framework of scaling invariance, the virial theorem is derived from the RMF [7, 8] Hamiltonian in the relativistic Thomas–Fermi (RTF) and relativistic extended Thomas–Fermi (RETF) approximations [9–11, 12–16]. For the sake of thoroughness, we briefly describe a number of key expressions that are essential to the current computations. The non-linear Lagrangian proposed by Boguta and Bodmer [17] was utilized to examine many-body correlations arising from the non-linear components in the σ-meson self-interaction. The Hamiltonian for the relativistic mean-field nucleon-meson interacting system is written as [7–11, 18]:

$$\begin{aligned}\mathcal{H} = \sum_i \varphi_i^\dagger \left[-i\vec{\alpha}\cdot\vec{\nabla} + \beta m^* + g_v V + \frac{1}{2} g_\rho R\tau_3 + \frac{1}{2} e\mathcal{A}(1+\tau_3)\right]\varphi_i + \frac{1}{2}\left[(\vec{\nabla}\phi)^2 + m_s^2\phi^2\right] \\ + \frac{1}{3} b\phi^3 + \frac{1}{4} c\phi^4 - \frac{1}{2}\left[(\vec{\nabla}V)^2 + m_v^2 V^2\right] - \frac{1}{2}\left[(\vec{\nabla}R)^2 + m_\rho^2 R^2\right] - \frac{1}{2}(\vec{\nabla}\mathcal{A})^2\end{aligned} \quad (1)$$

The fields for the σ, ω, ρ−mesons, and photon are ϕ, V, and A, respectively. The τ_3 is the 3^{rd} component of the iso-spin of the ρ−meson. The actual mass m of the nucleon appears to be missed due to its oscillations in the mesonic medium and acquires the effective mass $m^* = m - g_s\phi$. The m_s, m_v, and m_ρ are the masses for the σ−, ω−, and ρ−mesons, respectively. The coupling constants g_s, g_v, g_ρ, and $e^2/4\pi=1/137$ correspond to the σ, ω, ρ-mesons and photon couplings with the nucleons, respectively. The b and c are self-couplings for the non-linear σ − ω model for the σ−meson field. Using the variational principle, the equations of motion for the nucleons and meson fields can be derived. In the semi-classical approximation, in terms of density, the Hamiltonian is given by:

$$\mathcal{H} = \mathcal{E} + g_v V\rho + g_\rho R\rho_3 + e\mathcal{A}\rho_p + \mathcal{H}_f, \quad (2)$$

with,

$$\mathcal{E} = \sum_i \varphi_i^\dagger\left[-i\vec{\alpha}\cdot\vec{\nabla} + \beta m^*\right]\varphi_i \quad (3)$$

Here, H_f is the free part of the Hamiltonian, and the total density ρ is the sum of the proton ρ_p and neutron ρ_n density distributions.

The harmonic oscillator equation $E_{c.m.} = \frac{3}{4}\left(41A^{-1/3}\right)$is used to define the correction factor from the center of mass (c.m.) kinetic energy, where A is the mass number of the nucleus.

The following are the root mean square charge radius (R_{ch}), proton radius (R_p), neutron radius (R_n), and matter radius (R_{rms}):

$$< R_p^2 >= \frac{1}{Z}\int \rho_p(r_\perp, z) r_p^2 d\tau_p \tag{4}$$

$$< R_n^2 >= \frac{1}{N}\int \rho_n(r_\perp, z) r_n^2 d\tau_n \tag{5}$$

$$R_{ch} = \sqrt{R_p^2 + 0.64} \tag{6}$$

$$< R_{rms}^2 >= \frac{1}{A}\int \rho(r_\perp, z) r^2 d\tau \tag{7}$$

Here, all terms have their usual meanings. The total binding energy of the system and other observables can be obtained from standard relations [19–21].

RESULTS AND DISCUSSIONS

The Binding Energy and Two-Neutron Separation Energy

Nuclear Physics research relies heavily on the binding energy (BE) of finite nuclei. Of all the known nuclear observables, this quantity can be measured with the highest degree of accuracy. Knowing the computed BE and the extent to which the approach can be replicated is, therefore, very revealing. We calculated the BE for superheavy nuclei Z = 122 with neutron range N = 174 − 216.

In an isotopic series, the BE reflects nuclear stability and provides an estimate of the energy required to separate a neutron. We provide the BE results of our calculations for superheavy nuclei Z = 122 using the RETF framework with the NL3 parameter set. We compare our obtained results with the well-established theoretical finite-range droplet model (FRDM) model [22]. In addition to FRDM data, we also compare our results with the relativistic Hartree calculation by taking the same NL3 parameter set [6]. The results obtained are presented in the Table 2 and in the upper panel of Figure 1.

The table indicates that for almost all isotopes considered in the mass region of RETF, we typically observe a consistent over-BE of approximately 44 MeV. In other words, RETF formalism produces a BE that is approximately 1% greater than that of the FRDM data. A scaling technique can be applied to close the BE gap between the FRDM and RETF methods, with $f_s \approx 1.026$, indicating that the exact FRDM binding energy can be calculated by dividing the RETF binding energy values by f_s.

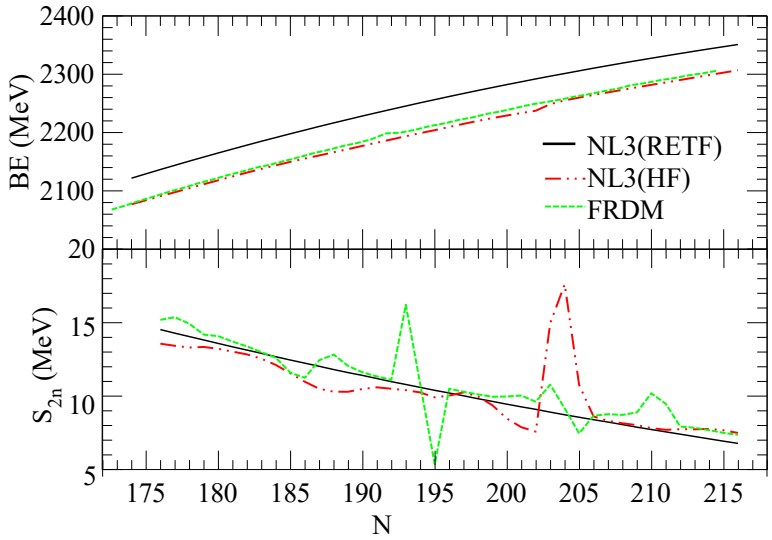

Figure 1. The binding energy (BE) obtained from the relativistic extended Thomas–Fermi (RETF) [11] (black color) calculations for some selected nuclei is compared with the relativistic Hartree–Fock (RHF) [6] (red color), as well as compared with the FRDM data (green color) [22]. The energy is in MeV.

The Hartree–Fock (HF) calculation provides lower predictions than the RETF results. The RMF-HF values for BE vary from the FRDM results by approximately 8 MeV. In an isotopic series, the calculations of the BE toward the neutron dripline increase steadily with the number of neutrons and become more rigid with the total number of atoms.

The two-neutron separation energy S_{2n} can be calculated with the formula below:

$$S_{2n} = BE(N, Z) - BE(N - 2, Z - 2) \quad (8)$$

The nuclear binding energy, indicated by the atomic number Z and neutron number N, is expressed as BE (N, Z). A sudden decrease in S_{2n} along an isotopic chain, as shown in the lower panel of Figure 1, indicates a magic neutron number, supporting the concept of shell closure within the nuclear shell model. We observed a significant peak at N = 203 in our assessment of the NL3 with the RETF force parameter, which resembled the peak identified in our analysis of the NL3 with the HF force parameter at N = 193. This shows the enhanced stability of nuclei concerning the decay of two neutrons.

R_{ch} and R_{rms} Radius of Super Heavy Nuclei $Z = 122$

This section investigates the charge radius and the root mean square (rms) radius for nuclei in the isotopic range of Z = 122. The rms charge radius R_{ch} and the rms matter distribution radius R_{rms} for isotopes Z = 122 are shown in Figure 2. We concentrate on the charge radius of Z = 122 isotopes in the upper part of the image. The nuclear charge radius is a key observable that helps characterize the nuclear shell model and provides an understanding of the impact of interactions on the nuclear structure. The results of the NL3 force parameter with RETF were compared with R_{ch}, which was determined using the HF method.

The values calculated for R_{ch} and R_{rms} are shown in Table 1 and Figure 2. In our calculation, R_{ch} and R_{rms} constantly increase with increasing neutron number N = 174 − 216. In the upper panel of the Figure 2, we observed that R_{ch} intersects at neutron number N = 175 in both of our calculations. A steady rise is noted from N = 174 − 177, followed by a sudden drop to neutron number N = 209.

Relative to the NL3 force parameter with RETF, a sharp decline is observed up to neutron number N = 193, and a constant increase is observed up to neutron number N=201, reaching a maximum at neutron number N = 205, followed by a steady increase in charge up to neutron number N = 216.

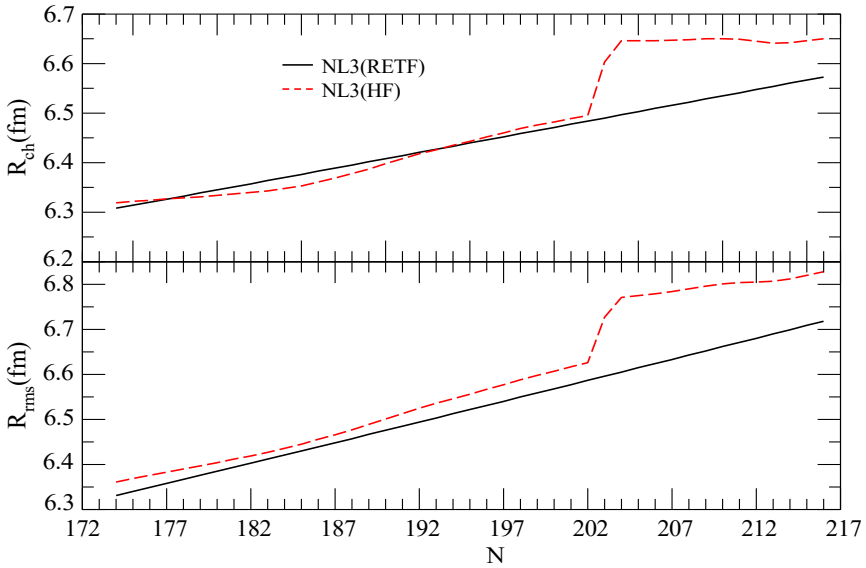

Figure 2. The root mean square charge radius R_{ch} and matter distribution radius R_{rms} obtained from the relativistic extended Thomas–Fermi (RETF) [11] (black color) for some selected nuclei are compared with the relativistic Hartree–Fock (HF) [6]. The radius is in (fm).

Table 1. The binding energy (BE) obtained from the relativistic extended Thomas–Fermi (RETF) [11] calculations for some selected nuclei is compared with the relativistic Hartree–Fock (RHF) [6] as well as with the available FRDM data [22]. The energy is in MeV.

Nucleus	ETF (BE)	HF (BE)	FRDM (BE)	Nucleus	ETF (BE)	HF (BE)	FRDM (BE)
174	2121.69	2076.86	2068.61	175	2129.17	2083.82	2075.86
176	2136.53	2090.78	2084.07	177	2143.78	2097.6	2091.49
178	2150.92	2104.45	2099.28	179	2157.95	2111.31	2106
180	2164.87	2118.04	2113.69	181	2171.68	2124.72	2120.06
182	2178.39	2131.27	2127.44	183	2184.99	2137.67	2133.44
184	2191.48	2143.82	2140.46	185	2197.87	2149.68	2145.5
186	2204.16	2155.29	2152.19	187	2210.35	2160.7	2158.36
188	2216.43	2166.12	2165.42	189	2222.42	2171.53	2170.85
190	2228.32	2177.13	2177.5	191	2234.11	2182.64	2182.67
192	2239.81	2188.15	2189.1	193	2245.42	2193.57	2199.1
194	2250.93	2198.93	2200.4	195	2256.35	2204.04	2205.26
196	2261.69	2209.51	2211.43	197	2266.93	2214.83	2216.09
198	2272.08	2220.03	2222.09	199	2277.15	2224.79	2226.6
200	2282.12	2229.13	2232.62	201	2287.02	2233.34	2237.19
202	2291.83	2237.39	2242.81	203	2296.55	2248.57	2248.48
204	2301.19	2255.13	2252.57	205	2305.75	2259.83	2256.63
206	2310.23	2264.37	2261.86	207	2314.64	2268.79	2266.02
208	2318.96	2273.17	2271.2	209	2323.2	2277.47	2275.52
210	2327.37	2281.66	2281.94	211	2331.46	2285.85	2285.58
212	2335.48	2290.08	2290.53	213	2339.42	2294.26	2294.1
214	2343.29	2298.52	2298.89	215	2347.08	2302.61	2302.29
216	2350.81	2306.7	2306.95				

The matter radius distributions (encompassing protons and neutrons) for the NL3 force parameter with RETF and HF sets are depicted in the lower part of Figure 2. Our analysis shows that the rms radii grow until neutron number N = 202. A sharp-like structure is observed at the neutron number N = 202, then experiences a sharp rise at neutron number N = 205. A consistent rise is observed from N = 205 − 208, succeeded by a sudden decline at neutron number N = 209. Thereafter, a consistent rms radius is upheld until the neutron number N = 216. Surface/volume saturation leads to a rise in symmetry energy, as demonstrated by the neutron skin thickness, arising from the surplus neutrons and increasing linearly with the neutron number. The symmetry energy component in the nuclear equation of state (EoS), which defines the disparity between the count of neutrons and protons, influences the neutron skin-thickness ΔR_{np}. It reveals the distributions of nucleons and the forces within a nucleus. In nuclear structure and neutron star physics, the symmetry energy of nuclei is essential.

The equation for the neutron skin thickness is given by

$$\Delta R_{np} = < R_n^2 >^{1/2} - < R_p^2 >^{1/2} \quad (9)$$

Where, R_n represents the root mean square radii of neutrons, while R_p signifies the radii of neutrons and protons, respectively. Figure 3 illustrates the obtained data on the neutron skin thickness. As shown in Figure 3, the neutron skin thickness linearly increases with an increase in the neutron number. This is consistent with the calculations from the HF. A notable kink was observed at neutron number N = 194 in the HF calculation.

Table 2. The root mean square charge radius (R_{ch}) and root mean square matter distribution radius (R_{rms}) obtained from the relativistic extended Thomas–Fermi (RETF) [11] calculations for some selected nuclei are compared with the relativistic Hartree–Fock (HF) [6]. The radius is in *fm*.

Nucleus R_{ch}	(RETF) Rch	(HF) R_{rms}	(RETF) Rrms	(HF)	NucleusR_{ch}	(RETF) Rch	(HF)R_{rms}	(RETF)	R_{rms} (HF)
174	6.308	6.319	6.331	6.361	175	6.314	6.322	6.34	6.369
176	6.32	6.324	6.349	6.376	177	6.326	6.327	6.358	6.383
178	6.332	6.329	6.367	6.39	179	6.339	6.331	6.376	6.397
180	6.345	6.334	6.385	6.404	181	6.351	6.337	6.394	6.412
182	6.357	6.34	6.403	6.419	183	6.364	6.343	6.412	6.427
184	6.37	6.348	6.421	6.436	185	6.376	6.353	6.43	6.445
186	6.383	6.361	6.439	6.456	187	6.389	6.369	6.448	6.466
188	6.395	6.378	6.457	6.477	189	6.402	6.387	6.467	6.489
190	6.408	6.398	6.476	6.501	191	6.414	6.408	6.485	6.513
192	6.421	6.418	6.494	6.525	193	6.427	6.426	6.503	6.536
194	6.433	6.435	6.513	6.546	195	6.44	6.443	6.522	6.556
196	6.446	6.452	6.531	6.567	197	6.452	6.46	6.54	6.577
198	6.459	6.469	6.55	6.588	199	6.465	6.476	6.559	6.598
200	6.471	6.482	6.568	6.607	201	6.478	6.489	6.577	6.617
202	6.484	6.495	6.587	6.626	203	6.49	6.603	6.596	6.727
204	6.497	6.646	6.605	6.771	205	6.503	6.646	6.615	6.775
206	6.51	6.646	6.624	6.779	207	6.516	6.647	6.633	6.784
208	6.522	6.648	6.643	6.79	209	6.529	6.65	6.652	6.796
210	6.535	6.65	6.662	6.801	211	6.541	6.649	6.671	6.804
212	6.548	6.645	6.68	6.805	213	6.554	6.641	6.69	6.807
214	6.561	6.642	6.699	6.812	215	6.567	6.646	6.709	6.820
216	6.573	6.65	6.718	6.828					

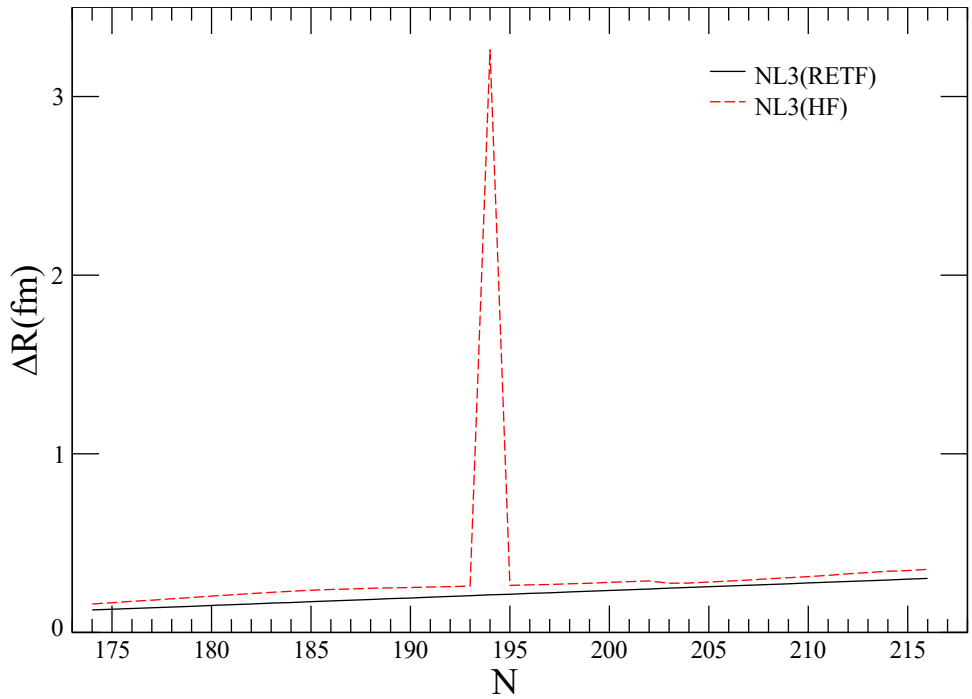

Figure 3. The neutron skin thickness obtained from the relativistic extended Thomas–Fermi (RETF) [11] (black color) calculations for some selected nuclei is compared with the relativistic Hartree–Fock (RHF) [6] (red color). The neutron skin thickness is in fm.

The $Q\alpha$ Energy and α-Decay Half-Life T^{α} of a SUPER HEAVY Nuclei

To determine the half-life of α particles, referred to as T^{α}, it is important to take into account: It is essential to determine the nuclear energy Q_{α}. The concepts of parent and daughter isotopes, as well as an understanding of the BE associated with their relationship, are essential. The energy of the α particle, particularly the binding energy of ^{4}He, must be considered. This energy can be obtained from observational data when available. The previously mentioned factors are also relevant to different mass formulas and the relativistic mean-field Lagrangian approach. The energy Q_{α} can be approximated using the following equation [23]:

$$Q_{\alpha}(N, Z) = BE(N, Z) - BE(N - 2, Z - 2) - BE(2, 2) \quad (10)$$

In this equation, BE (N, Z), BE (N − 2, Z − 2), and BE (2, 2) denote the corresponding binding energies, respectively. The parent and daughter isotopes, along with the He nucleus, have a binding energy of 28.296 MeV. In this context, N represents the number of neutrons, and Z indicates the number of protons.

Having the Q_{α}−values of nuclei, we can approximately evaluate the α-decay half-lives $\log_{10} T^{\alpha}_{1/2}(s)$$\log_{10}T^{\alpha}$(s) for different nuclei employing the phenomenological equation by Viola and Seaborg [24]:

$$\log_{10} T^{\alpha}_{1/2}(s) = \frac{(aZ-b)}{\sqrt{Q_{\alpha}}} - (cZ + d) + h_{log} \quad (11)$$

We refer to papers [24–26] for the values of parameters and other significant observable quantities connected to Qα and the half-life of α decay for a suitable explanation.

Figure 4 in the left panel shows the Q_{α} value obtained from the RMF calculation of the force parameter NL3 with RETF for isotope Z = 122 as a solid black line. Furthermore, the results are compared with the force parameter NL3 within the HF, represented by the dotted line, and the available FRDM data (green dotted line). Although the Qα values are in good agreement, it is important to note that the exponential component of α in the $T_{1/2}$(s) value can cause significant variations in the values. Therefore, it is better to compare $\log_{10} T^{\alpha}_{1/2}(s)$ values instead of $T^{\alpha}_{1/2}(s)$ values.

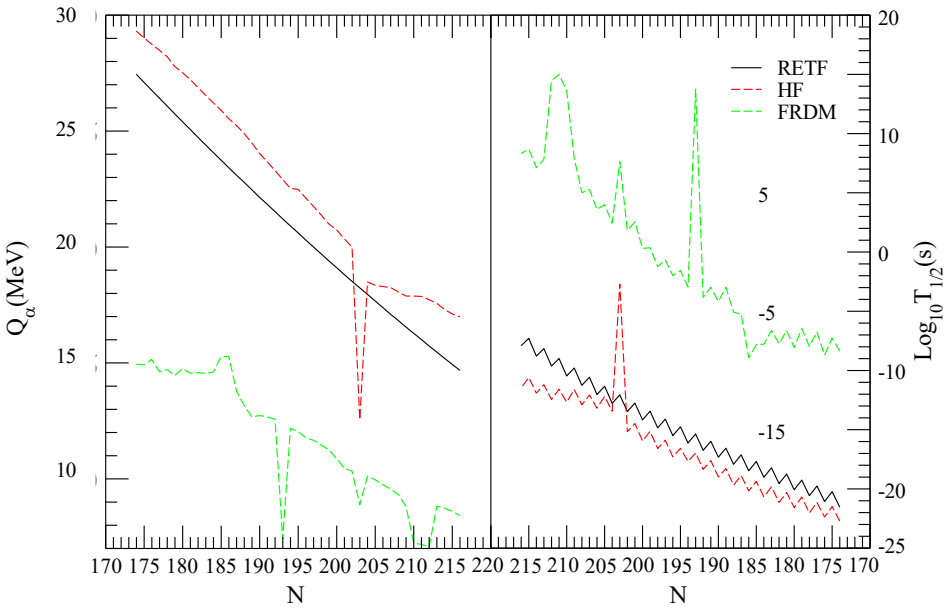

Figure 4. The Q_{α} and the Half-life time $T_{1/2}$ of the α−decay are obtained from the relativistic extended Thomas–Fermi (RETF) [11] (black color) calculations for some selected nuclei, and are compared with the relativistic Hartree–Fock (RHF) [6] as well as compared with the FRDM (green color) [22]. The $Q\alpha$ energy is in MeV and $T_{1/2}$ is in second(s).

The results obtained for $T_{1/2}^{\alpha}(s)$ are shown in the right panel of Figure 4 and are comparable to the FRDM data for the NL3 force parameter within the HF, demonstrating the robustness of the linearly decreasing with increasing neutron number. In our calculations, Qα linearly decreases with an increase in the neutron number. This indicates that these isotopes are completely stable in the alpha-decay mode and follow different decay modes, such as spontaneous fission (SF) and beta decay (BD), with NL3 parameters.

However, alpha-decay, SF, and BD can occur in the FRDM and NL3 force parameters. The overall isotopic stability trend Z = 122 increases with the number of neutrons. The results obtained are comparable with the HF and FRDM results. To obtain a more accurate conclusion, it is necessary to calculate other decay modes such as SF and BD.

SUMMARY AND CONCLUSION

Z = 122 isotopes with neutron counts N = 174 − 216 have been analyzed for their ground-state bulk properties using the RMF approach. The calculations are executed utilizing the most effective NL3 force parameter alongside the RETF and HF configurations. The outcomes derived from RETF and HF are compared with the FRDM data. The fundamental state characteristics are examined thoroughly, encompassing the BE, two-neutron separation energy, charge radius, rms radius distributions, and neutron skin thickness. We achieved a magic number at N=204 in the NL3 force parameter computations using HF. We found another magic number at N=194 in the FRDM calculations, which is absent from both RETF and HF results. We got a kink in the neutron skin thickness distribution, which is totally absent in the RETF approach. So, for a more fundamental study, we must extend our calculation for deformed cases and must consider more decay modes like SF and BD.

REFERENCES

1. Manjunatha HC, Nagaraja AM, Gupta PSD, Manjunatha N, Sowmya N, Raj SAC. Heavy particle radioactivity of superheavy element Z=122. Phys Part Nucl Lett. 2022;19(5):597-605. doi:10.1134/S1547477122050260.
2. Godbey K, Nunes FM, Albertsson M, Cook KJ, Gates JM, Hagel K, et al. Paths to superheavy nuclei. J Phys G Nucl Part Phys. 2025;52(12):120501. doi:10.1088/1361-6471/ae198f.
3. Shen WQ, Albinski J, Gobbi A, Gralla S, Hildenbrand KD, Herrmann N, et al. Fission and quasifission in U-induced reactions. Phys Rev C. 1987;36(1):115–142. doi:10.1103/PhysRevC.36.115. PMID: 9954057.
4. Itkis MG, Beghini S, Bogachev AA, Corradi L, Dorvaux O, Gadea A, et al. Shell effects in fission and quasi-fission of heavy and superheavy nuclei. Nucl Phys A. 2004;734:136-147. doi:10.1016/j.nuclphysa.2004.01.022.
5. Manjunatha HC. Theoretical prediction of probable isotopes of superheavy nuclei of Z=122. Int J Mod Phys E. 2016;25(11):1650100. doi:10.1142/S0218301316501007.
6. Lalazissis GA, König J, Ring P. New parametrization for the Lagrangian density of relativistic mean field theory. Phys Rev C. 1997;55(1):540–543. doi:10.1103/PhysRevC.55.540.
7. Piekarewicz J. Correlating the giant-monopole resonance to the nuclear-matter incompressibility. Phys Rev C. 2002;66(3):034305. doi:10.1103/PhysRevC.66.034305.
8. Serot BD, Walecka JD. Relativistic nuclear many-body theory. In: Ainsworth TL, Campbell CE, Clements BE, Krotscheck E, editors. Recent Progress in Many-Body Theories. Boston (MA): Springer US; 1992. p. 49-92. doi:10.1007/978-1-4615-3466-2_5.
9. Patra SK, Centelles M, Viñas X, Del Estal M. Scaling in relativistic Thomas-Fermi approach for nuclei. Phys Lett B. 2001;523(1-2):67-72. doi:10.1016/S0370-2693(01)01328-4.
10. Patra SK, Viñas X, Centelles M, Del Estal M. Scaling calculation of isoscalar giant resonances in relativistic Thomas-Fermi theory. Nucl Phys A. 2002;703(1-2):240-268. doi:10.1016/S0375-9474(01)01531-7.
11. Zhu C, Qiu XJ. A study of the giant monopole state within the relativistic Thomas-Fermi approximation. J Phys G Nucl Part Phys. 1991;17(2):L11–L17. doi:10.1088/0954-3899/17/2/002.

12. Centelles M, Viñas X, Barranco M, Schuck P. A semiclassical approach to relativistic nuclear mean field theory. Ann Phys (N Y). 1993;221(1):165-204. doi:10.1006/aphy.1993.1007.
13. Centelles M, Viñas X, Barranco M, Marcos S, Lombard RJ. Semiclassical approximations in non-linear σω models. Nucl Phys A. 1992;537(3-4):486-500. doi:10.1016/0375-9474(92)90365-Q.
14. Joubert D. Density Functionals: Theory and Applications. Proceedings of the Tenth Chris Engelbrecht Summer School in Theoretical Physics; 1997 Jan 19–29; Meerensee, near Cape Town, South Africa. (Lecture Notes in Physics; vol. 500). Berlin: Springer-Verlag; 1998.
15. Centelles M, Del Estal M, Viñas X. Semiclassical treatment of asymmetric semi-infinite nuclear matter: Surface and curvature properties in relativistic and non-relativistic models. Nucl Phys A. 1998;635(1-2):193-230. doi:10.1016/S0375-9474(98)00167-5.
16. Centelles M, Viñas X, Barranco M, Ohtsuka N, Faessler A, Khoa DT, et al. Relativistic extended Thomas-Fermi calculations of finite nuclei with realistic nucleon-nucleon interactions. Phys Rev C. 1993;47(3):1091–1102. doi:10.1103/PhysRevC.47.1091. PMID: 9968543.
17. Boguta J, Bodmer AR. Relativistic calculation of nuclear matter and the nuclear surface. Nucl Phys A. 1977;292(3):413-428. doi:10.1016/0375-9474(77)90626-1.
18. Centelles M, Patra SK, Roca-Maza X, Sharma BK, Stevenson PD, Viñas X. The influence of the symmetry energy on the giant monopole resonance of neutron-rich nuclei analyzed in Thomas-Fermi theory. J Phys G Nucl Part Phys. 2010;37(7):075107. doi:10.1088/0954-3899/37/7/075107.
19. Gambhir YK, Ring P, Thimet A. Relativistic mean field theory for finite nuclei. Ann Phys (N Y). 1990;198(1):132-179. doi:10.1016/0003-4916(90)90330-Q.
20. Pattnaik JA, Naik KC, Panda RN, Bhuyan M, Patra SK. Structure and reaction studies of Z=120 isotopes using non-relativistic and relativistic mean-field formalisms. Pramana. 2023;97(3):136. doi:10.1007/s12043-023-02619-9.
21. Patra SK, Praharaj CR. Relativistic mean field study of light medium nuclei away from beta stability. Phys Rev C. 1991;44(6):2552–2565. doi:10.1103/PhysRevC.44.2552. PMID: 9967691.
22. Möller P, Sierk AJ, Ichikawa T, Sagawa H. Nuclear ground-state masses and deformations: FRDM(2012). At Data Nucl Data Tables. 2016;109-110:1-204. doi:10.1016/j.adt.2015.10.002.
23. Patra SK, Praharaj CR. Q values for α-decays in the superheavy element chain. J Phys G Nucl Part Phys. 1997;23(8):939–950. doi:10.1088/0954-3899/23/8/008.
24. Viola VE Jr, Seaborg GT. Nuclear systematics of the heavy elements-II. Lifetimes for alpha, beta and spontaneous fission decay. J Inorg Nucl Chem. 1966;28(3):741-761. doi:10.1016/0022-1902(66)80412-8.
25. Duarte SB, Tavares OAP, Guzmán F, Dimarco A, García F, Rodríguez O, et al. Half-lives for proton emission, alpha decay, cluster radioactivity, and cold fission processes calculated in a unified theoretical framework. At Data Nucl Data Tables. 2002;80(2):235–299. doi:10.1006/adnd.2002.0881.
26. Le NN, Duy NN. Examination of α-decay half-lives of undetected transfermium isotopes. Int J Mod Phys E. 2020;29(10):2050085. doi:10.1142/S0218301320500858.

